Supporting information for the paper:

Ag_9 quantum cluster through a solid state route

Thumu udaya B. Rao, Boodeppa Nataraju, Thalappil Pradeep *

DST Unit on Nanoscience (DST-UNS), Department of Chemistry and Sophisticated Analytical Instrument Facility, Indian Institute of Technology Madras, Chennai 600 036, India

*E-mail: pradeep@iitm.ac.in

Table of contents

S1. Supporting information 1

Experimental Section

Synthesis of $Ag_9(H_2MSA)_7$: About 47 mg of $AgNO_3$(s) was added to 187 mg of H_2MSA(s) at room temperature and the mixture was ground well until a conversion of color from colorless to orange occurred. About 50 mg $NaBH_4$ was added and grinding was continued for 10 more min and then 15 mL of water was added slowly (in one mL steps) resulting in the formation of a reddish brown solution. Clusters were precipitated immediately by the addition of excess ethanol. The resulting precipitate was collected and washed repeatedly with ethanol through centrifugal precipitation. Finally, the Ag@(H_2MSA) precipitate was dried and collected as a reddish brown powder. The dried product was stored in the laboratory atmosphere. Yield of crude $Ag_9(H_2MSA)_7$ was 60 mg, starting from the above method.

Ag(I)MSA was prepared following the process reported by K. Nomiya.[1] Dissolving 47 mg of silver nitrate and 187 mg of H_2MSA in 1 mL of 1.5 M NaOH solution results in the formation of yellow colored oligomeric sodium salt of the silver(I)-thiolate complex. This stays in the solution. Powdered material was obtained by the evaporation of solvent by freeze drying. It was dissolved in D_2O and used for ^1H and ^{13}C NMR experiments.

Purification by polyacrylamide gel electrophoresis (PAGE): PAGE separation of the clusters was performed as per the procedure given below.

A gel electrophoresis unit with 1 mm thick spacer (Bio-rad, Mini-protein Tetra cell) was used to process the PAGE. The total contents of the acrylamide monomers were 28% (bis(acrylamide:acrylamide) = 7:93) and 3% (bis(acrylamide:acrylamide) = 6:94) for the separation and condensation gels, respectively. The eluting buffer consisted of 192 mM glycine and 25 mM tris(hydroxymethylamine). The crude mixture of Ag@(H_2MSA) clusters, as a reddish brown powder, obtained in the reaction was dissolved in 5% (v/v) glycerol-water solution (1.0 mL) at a concentration of 60 mg/mL. The sample solution (1.0 mL) was loaded onto a 1 mm gel and eluted for 4 h at a constant voltage of 150 V to achieve separation shown in Figure 1. The gel fractions containing the clusters were cut out, ground, and dipped in ice cold distilled water (2 mL) for 10 min. Subsequently, the solutions were centrifuged at 20,000 rpm for 5 min at -10 °C, followed by filtering with filter paper having 0.22 μm pores to remove the gel lumps suspended in the solution. The samples were freeze dried to get reddish brown (1st band) and red (2nd band) powders. First band shows the presence of plasmonic nanoparticles. The yield of the 2nd band was 20 mg.

We also performed high resolution electrophoresis using increased contents of acrylamide monomers of 35% (bis(acrylamide:acrylamide) = 7:93) and 3% (bis(acrylamide:acrylamide) = 6:94) for the separation and condensation gels, respectively. But, we did not observe any additional bands. Further increase in gel concentration and decrease of potential was not attempted in view of the decomposition of Ag_9.

Even without PAGE, the clusters are rather pure and the nanoparticle fraction can be removed by the addition of 70% ethanol followed by centrifugation. The clusters remain in solution.

Effect of solvents and ligands on the reaction: To check the effect of solvents, same concentrations were used as in the synthesis of $Ag_9(H_2MSA)_7$ cluster. The only change was, instead of 15 mL of water, the same amount of other solvents were added. To check the effect of various ligands, to the ground mixture of 1:5 mole ratio silver to thiol, 50 mg of sodium borohydride was added as in the earlier synthesis. The precipitated clusters were washed with ethanol to remove excess H_2MSA. The product was stored in nitrogen atmosphere.

Analytical procedures

A. UV-vis spectroscopy

Perkin Elmer Lambda 25 UV-vis spectrometer was used for the measurements. Spectra were typically measured in the range of 190-1100 nm.

B. Fourier-transform infrared (FT-IR) spectra

FT-IR spectra were measured with a Perkin Elmer Spectrum One instrument. KBr crystals were used as the matrix for sample preparation.

C. Luminescence spectroscopy

Luminescence measurements were carried out using HORIBA JOBIN VYON Nano Log instrument. The band pass for excitation and emission was set as 5 nm.

D. Transmission electron microscopy (TEM)

TEM images were collected using a JEOL 3010 microscope. A diluted solution was spotted on carbon coated copper grid and was dried in laboratory ambience. Images were collected at 200 keV, to reduce beam induced damage of the clusters. Our earlier studies had shown that small clusters are highly sensitive to electron beam and coalesce to yield nanoparticles on the grid.[2]

E. Electrospray ionization (ESI) mass spectrometry (MS)

The ESI MS measurements were done in the negative mode using an MDX Sciex 3200 QTRAP MS/MS instrument having a mass range of m/z 50-1700, in which the spray and the extraction are orthogonal to each other. The clusters, obtained after interfacial etching reaction and after PAGE separation, were dispersed in 1:1 water-methanol solution and used for mass spectrometric measurements. The samples were electrosprayed at a flow rate of 10 µL/min and ion spray voltage of 5 kV; the respective declustering potentials were -65 V and -50 V. The spectra were averaged for 100 scans. Spectra of crude samples were also measured similarly.

To clarify the presence of features due to the dissociation products and the absence of other preexisting cluster species in the mass spectrum (Figure 2), we have chosen an indirect method. We ascertained that some of the peaks present in the Ag_9 spectrum are in fact due to dissociation of the cluster to lower fragments. This is done by allowing as the cluster to decompose completely. As we discussed in the paper, the Ag_9 cluster decompose to form a pale yellow solution. This solution gives a featureless absorption spectrum in the UV-vis spectrum. To ensure the complete decomposition of Ag_9 clusters, the pale yellow solution was heated at 50 ^oC for 2 hours. We measured the ESI MS of this solution in water:methanol mixture. ESI MS spectra of the both the samples were identical. Importantly the peaks corresponding to Ag_9 cluster were absent, whereas the peaks assigned to dissociation products increased in intensity. This showed that the peaks assumed were indeed due to the dissociation of the Ag_9 cluster. Since the peaks after decomposition are identical to those of $Na_x[Ag_4(H_2MSA)_4]$- as observed by Nomiya et.al, we have taken the product to be oligomeric, anionic thiolato-silver(I) complex or silver thiolate.[1,3]

F. Matrix assisted laser desorption ionization time of flight mass spectrometry (MALDI TOF MS)

The mass spectrometric studies were conducted using a Voyager DE PRO Biospectrometry Workstation (Applied Biosystems) MALDI TOF MS instrument. A pulsed nitrogen laser of 337 nm was used (maximum firing rate: 20 Hz,

maximum pulse energy: 300 mJ) for desorption ionization and TOF was operated in the delayed extraction mode.

For laser desorption ionization (LDI) MS study, silver clusters were dispersed in water and directly spotted on the target plate. The sample was left to dry in air and inserted into the spectrometer.

Typical delay times employed were of the order of 75–150 ns. The mass spectra were collected in negative mode and were averaged for 100 shots. Most of the measurements were done in the reflectron mode. LDI studies were carried out to understand the gas phase clustering behavior.

The clusters were assigned by comparing their experimental and calculated isotope patterns. The spectra were simulated using the Data explorer version 4.0.0.0 software provided by Applied Biosystems Inc. which uses the isotope database of IUPAC.

G. SEM and EDAX analyses

Scanning electron microscopic (SEM) and energy dispersive X-ray (EDAX) analyses were done in a FEI QUANTA-200 SEM. For measurements, samples were drop-casted on an indium tin oxide coated conducting glass and dried in vacuum.

H. X-ray photoelectron spectroscopy

The photoelectron spectra of the samples were obtained using an ESCA probe/TPD of Omicron Nanotechnology. Sample in water was spotted on a Mo plate and allowed to dry in vacuum. The size of the analyzed area was about 3 mm^2. In view of the sensitivity of the sample, surface cleaning was not attempted. Al K_α radiation was used for excitation; a 180° hemispherical analyzer and a seven-channel detector were employed. The spectrometer was operated in the constant analyzer energy mode. Survey and high-resolution spectra were collected using pass energies of 50 and 20 eV, respectively. The pressure in the analyzer chamber was in the low 10^{-10} mbar range during spectrum collection. Binding energies of the core levels were calibrated with C 1s BE, set at 284.7 eV.

I. X-ray powder diffraction

Powder XRD patterns of the samples were recorded using PANalytical X'pertPro diffractometer. The powder samples of parent silver nanoparticles and clusters were taken on a glass plate and the X-ray diffractogram was collected in the 2Θ range of 5 to 100 degrees.

J. Thermogravimetry (TG) and Differential scanning calorimetry (DSC)

TG and DSC analyses of the pure clusters obtained after PAGE were carried out with a Perkin Elmer TGA 7 and Perkin Elmer DSC 7, respectively at a heating rate of 20 °C per min in N_2 atmosphere.

K. Raman spectroscopy

A Witec GmbH confocal Raman spectrometer, equipped with a Nd:YAG frequency doubled laser at 532 nm was used as the excitation source to collect the luminescence images. The laser was focused onto the sample using a 100X objective with the signal collected in a back scattering geometry. The signal, after passing through a super notch filter, was dispersed using a 150 grooves/mm grating onto a Peltier-cooled charge coupled device (CCD), which served as the detector. The sample mounted on a piezo stage was scanned with signals collected at every pixel. For the images displayed, the scan area was divided into 100X100 pixels for spectral image acquisition. Spectral intensities acquired over a predefined area were automatically compared to generate color-coded images. In the images, regions coded yellow are regions with maximum fluorescence intensities and regions shown in black are with minimum signal intensities. Luminescence masked the Raman spectrum.

L. NMR

Bruker AVANCE III 500 MHz (AV 500) multinuclei NMR was used for analyzing the samples. 20 mg/ 0.5 mL D_2O was used for ^{1}H and ^{13}C NMR analyses.

All the data presented in the paper are with the PAGE separated sample, except XPS, XRD and UV-Vis kinetics, for which the crude cluster sample was used. Several data were also collected with the crude sample as mentioned in the text.

M. Quantum yield

The quantum yield (QY) of the cluster was measured using rhodamine 6G (in water : MeOH) as a reference.

S2. Supporting information 2

Effect of addition of water

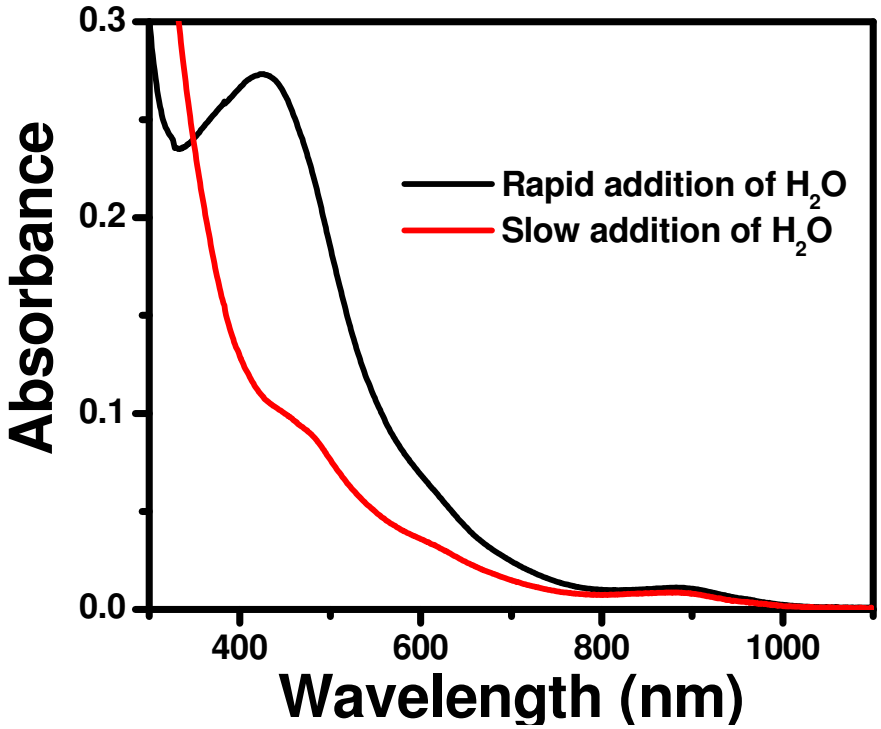

Figure S1. (A) UV-Vis spectra of the as synthesized crude mixtures at rapid and slow addition of water. Rapid addition makes silver nanoparticles showing surface plasmon resonance at 420 nm. Clusters are formed in rapid addition also.

S3. Supporting information 3

Effect of sequence of addition

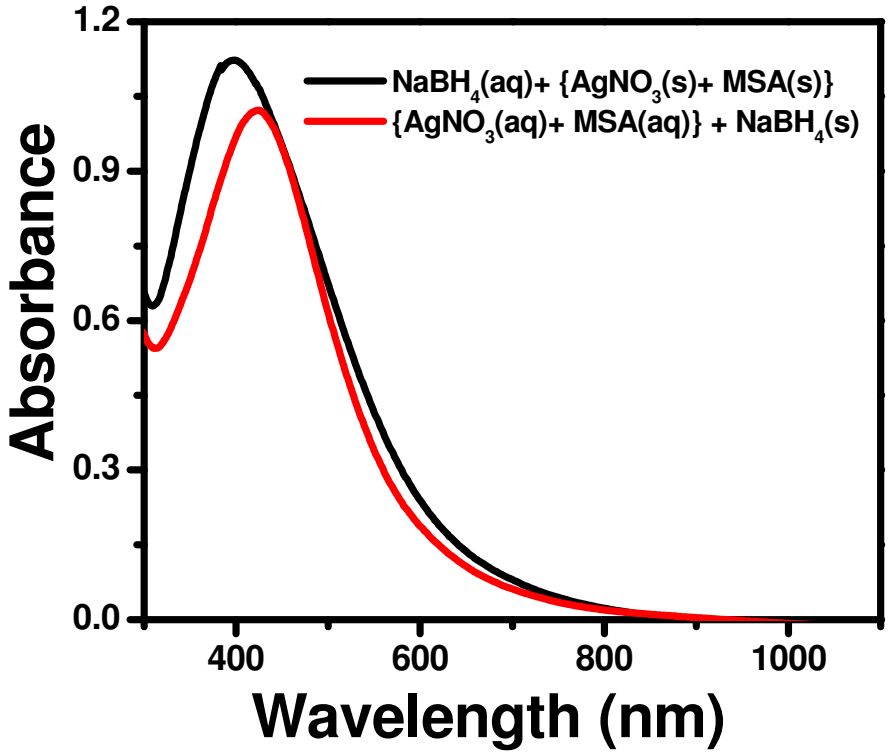

Figure S2. UV-Vis spectra of products formed in different types of syntheses. The addition sequence is indicated. Addition of reactants in the solid state is important to get clusters.

S4. Supporting information 4

Effect of $NaBH_4$ and Ag:thiol ratio

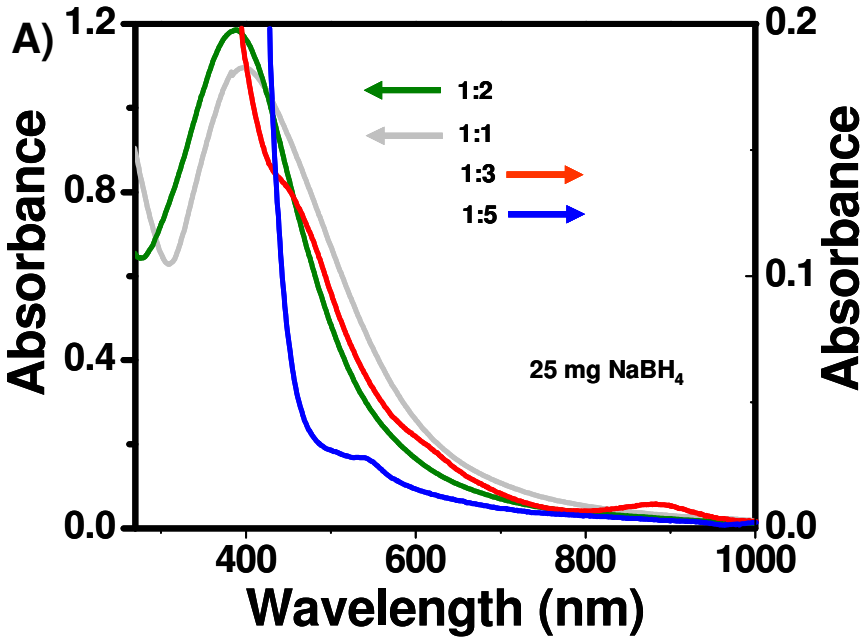

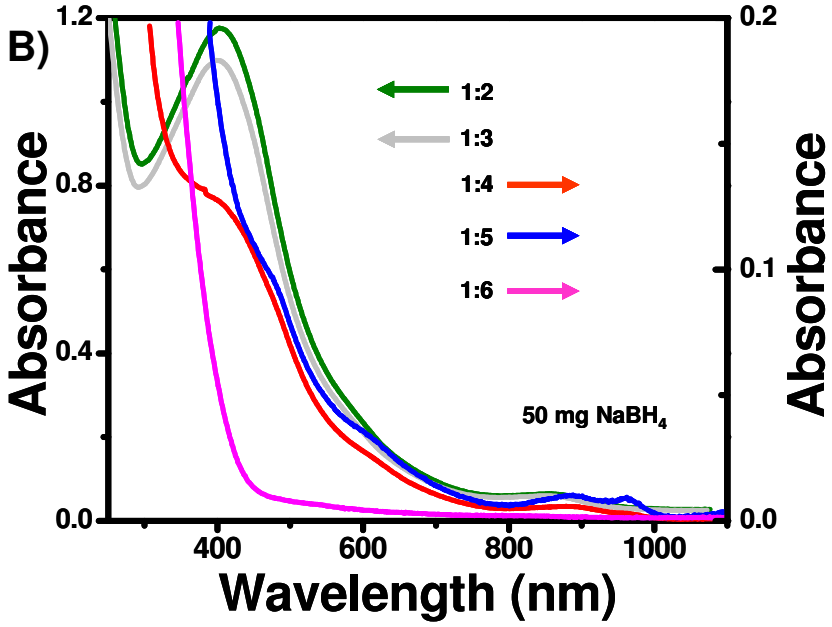

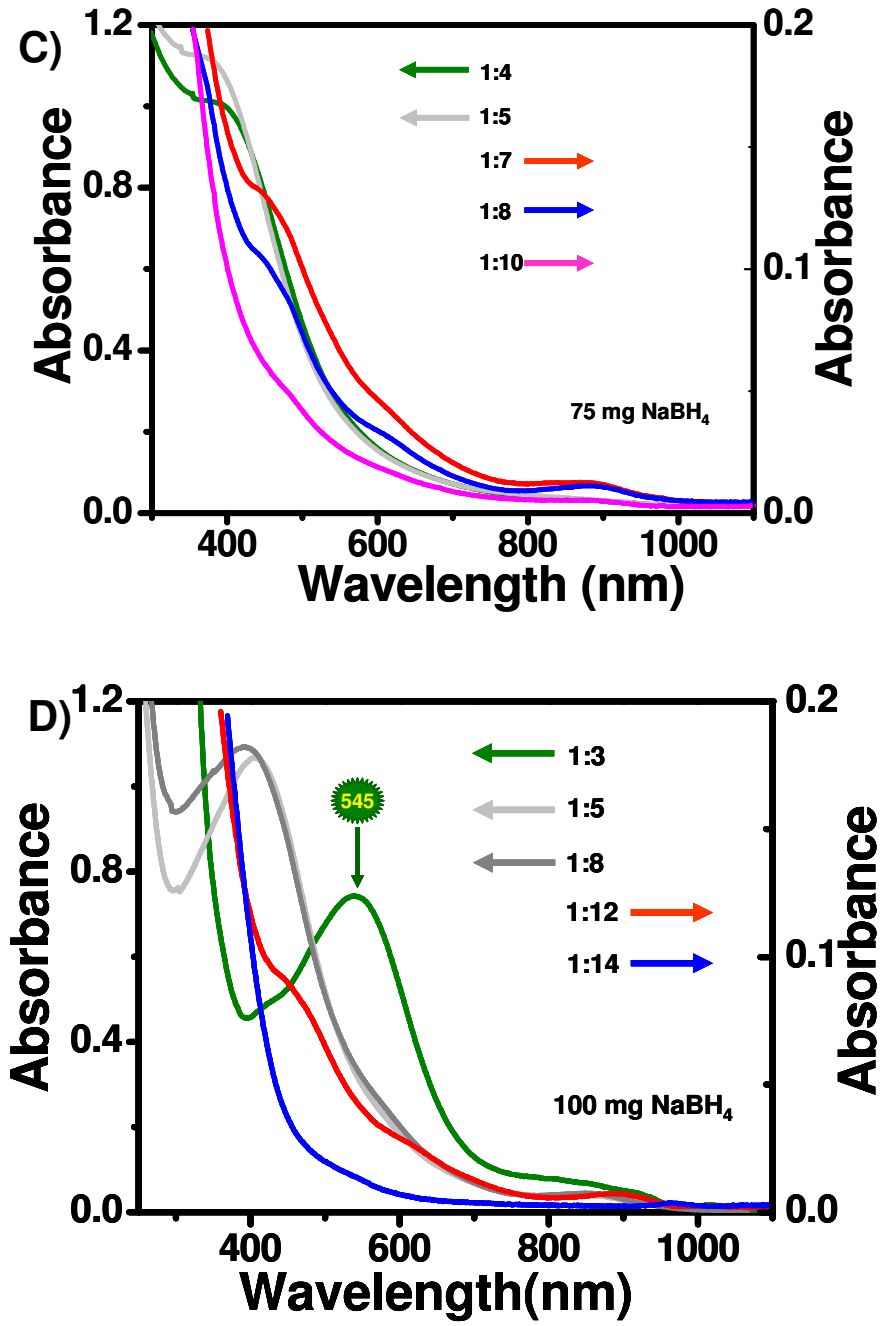

Figure S3. UV-Vis spectra of the as synthesized crude mixtures prepared at different mole ratios of silver to thiol ratio and at (A) 25 mg, (B) 50 mg, (C) 75 mg and (D) 100 mg of sodium borohydride. For certain traces, the y axis label is on the left and for others, the label is on the right. Color of the trace indicates the corresponding axes.

For these experiments, four different quantities of $NaBH_4$ in solid form such as 25, 50, 75 and 100 mg were added separately to solid mixtures of $AgNO_3$ and MSA, of varying molar ratio, from 1:0.5 to 1:12. Interesting variations in UV-vis spectra were observed. The data reveal that several factors influence the formation of the cluster. The molar ratio of silver to thiol was varying from 0.5 to 12. At lower concentrations of thiol, at a particular amount of $NaBH_4$, there is a tendency for the formation of nanoparticles, as expected. At an intermediate concentration of thiol,

formation of nanoclusters dominates. Yield of the cluster decreases upon further increasing the amount of thiol. At this stage, we expect that the main impurity may be silver-thiol complexes which have a featureless spectrum in its absorption profile. For silver to thiol ratios of 1:2 and 1:3, at 50 mg of $NaBH_4$, nanoparticles dominate. There is a sudden dampening in the intensity (by 1/10 th) at 400 nm and a new molecule-like absorption profile in 300-900 nm region appeared when thiol ratio was increased (1:5 and 1:6) at 50 mg $NaBH_4$. Optimal silver-to-thiol ratio for the formation of stable clusters is close to 1:5. This is far removed from the ratio in the product. It may note that for synthesizing $Au_{25}(SG)_{18}$ an initial gold:glutathione ratio of 1:4 is required whereas the stoichiometric ratio (1:0.72 = 25:18) would lead to the formation of nanoparticles.

The details of the figures are:

A) **In the case of 25 mg of $NaBH_4$**: $AgNO_3$:H_2MSA mole ratio 1:1, 1:2 gives a surface plasmon at 400 nm, showing the formation of nanoparticles. 1:4 mole ratio gives a step like behavior at 886, 625, 489 and 450 nm in the absorption profile, showing the formation of clusters, 1:4 mole ratio gives a peak at 540 nm. 1:6 gives a featureless spectrum showing the formation of complexes.

B) **In the case of 50 mg of $NaBH_4$**: $AgNO_3$:H_2MSA mole ratios of 1:2 and 1:3 give a surface plasmon at 400 nm, showing the formation of nanoparticles. 1:4 and 1:5 mole ratios give a step like behavior as mentioned in A). showing the formation of clusters. 1:6 gives a featureless spectrum showing the formation of complexes.

C**) In the case of 75 mg of $NaBH_4$**: $AgNO_3$:H_2MSA mole ratios of 1:4 and 1:5 give a surface plasmon at 400 nm, showing the formation of nanoparticles. 1:7 and 1:8 mole ratio give step like behavior as mentioned in A). showing the formation of clusters. 1:10 gives a featureless spectrum showing the formation of complexes.

C) **In the case of 100 mg of $NaBH_4$**: $AgNO_3$:H_2MSA mole ratios of 1:2 and 1:3 give a peak at 540 nm after several hours. 1:5, 1:6, 1:7, 1:8, 1:9, 1:10 and 1:11 give surface plasmon at 420 nm, showing the formation of nanoparticles. 1:12 mole ratio gives a step like behavior as mentioned in A). showing the formation of clusters. 1:14 gives a featureless spectrum showing the formation of complexes.

S5. Supporting information 5

Comparison of crude and PAGE separated clusters

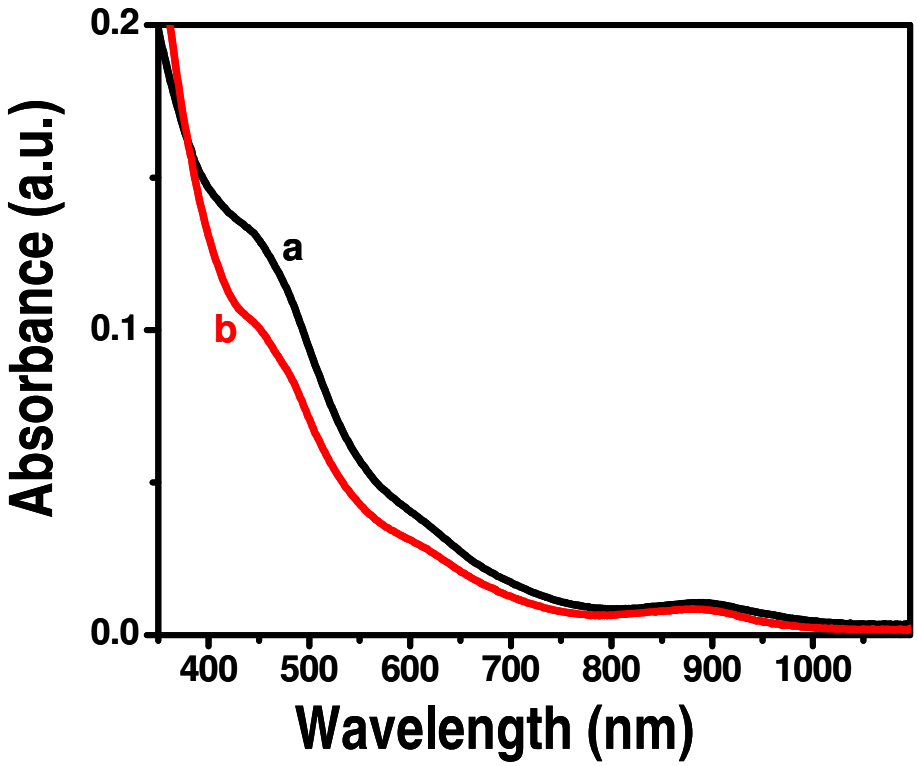

Figure S4. Comparison of the UV-Vis spectra of (a) as-synthesized cluster (before PAGE) and b) purified cluster (after PAGE).

S6. Supporting information 6

Luminescence spectra

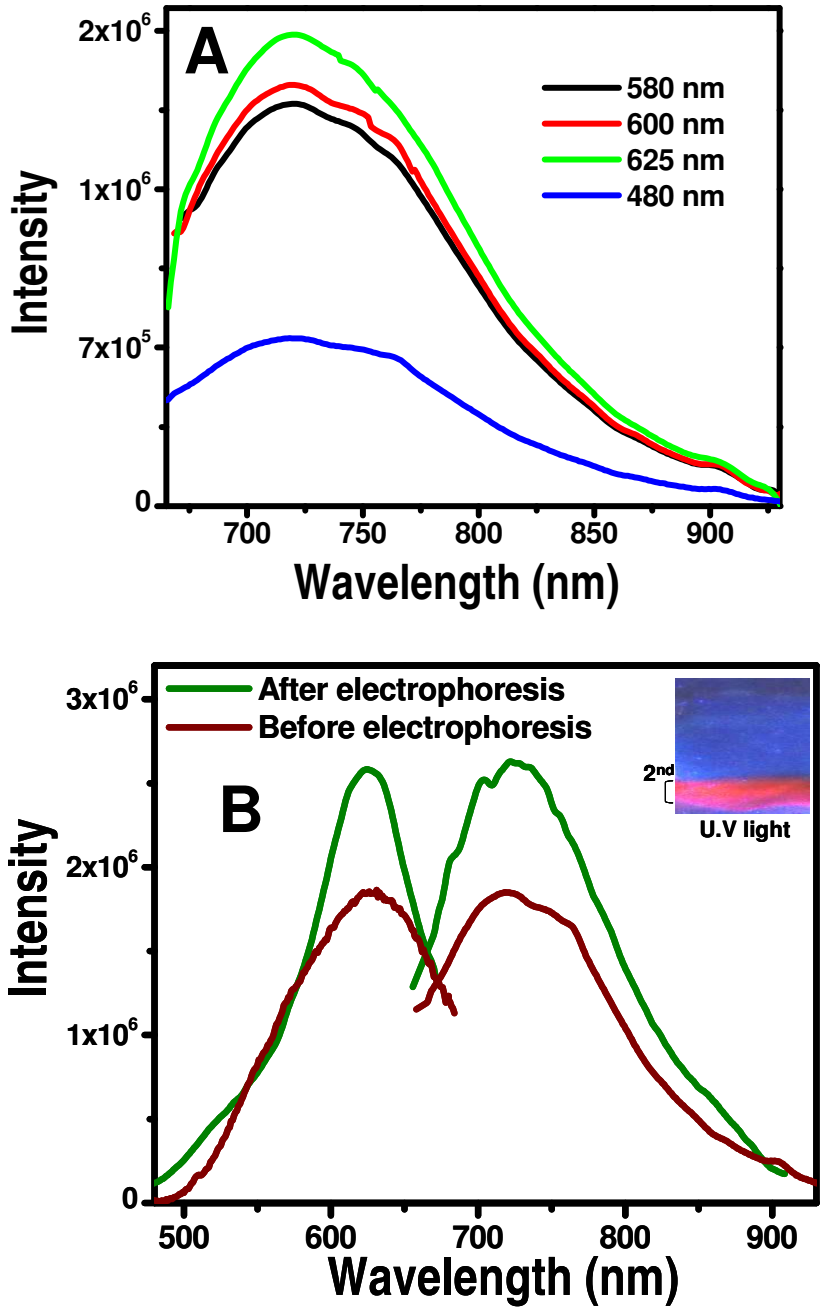

Figure S5. A) Luminescence spectra of the cluster in water: MeOH at different excitation wavelengths, the spectra are labeled using the excitation wavelength used. Emission at 720 nm is more intense at 625 nm excitation. B) Luminescence spectra of the cluster in water:MeOH mixture collected at ice cold temperature at the same concentrations. Photograph in the inset shows the gel after electrophoresis, in UV light, at RT. The cluster luminesces visibly even at RT. The first band does not appear in the UV light as it is composed of metallic nanoparticles which do not luminesce.

S7. Supporting information 7

Luminescence images of the solid with a Raman microscope

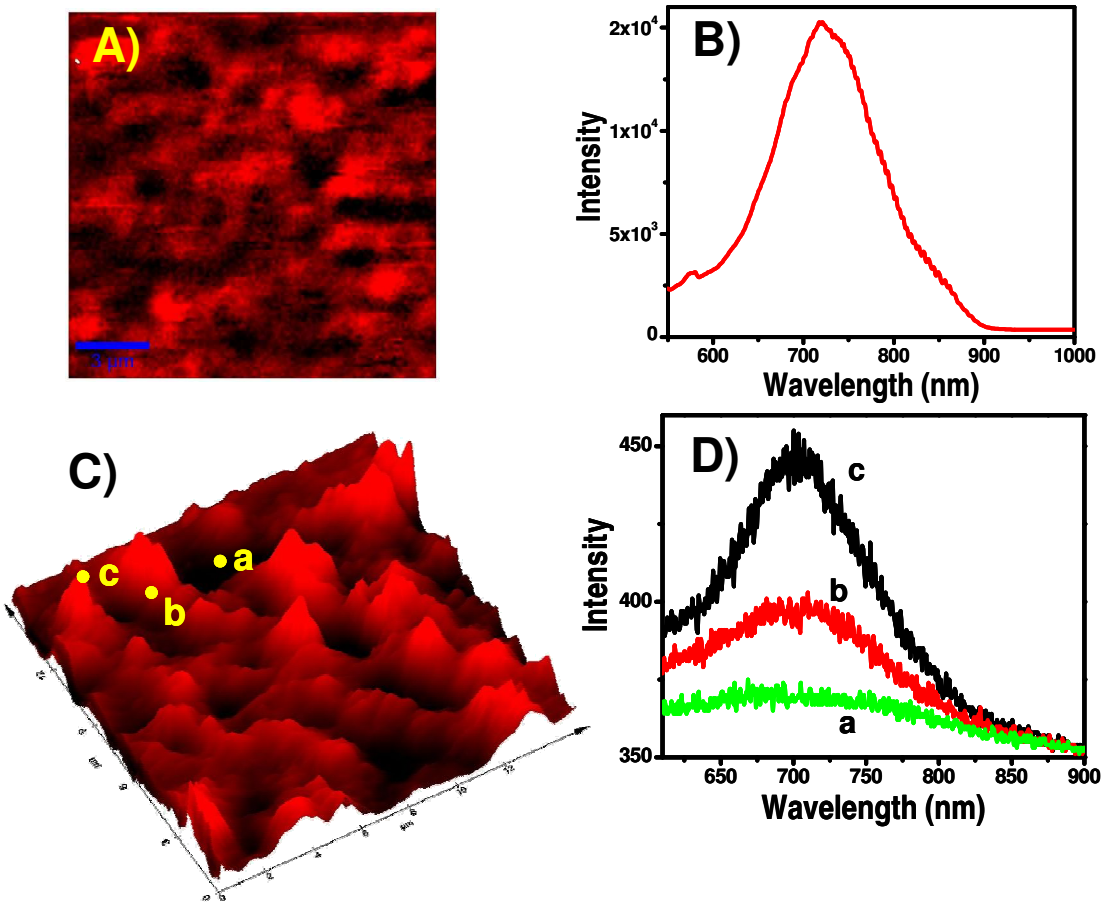

Figure S6. (A) Inherent luminescence image of the PAGE separated cluster collected by the spectroscopic mapping of an area 15 μm × 15 μm at an excitation wavelength of 532 nm. B) Solid state emission spectrum of the cluster, collected at 532 nm excitation. (C) 3D view of the image and (D) background luminescence profile from three different points a, b and c along the 3D image. Regions shown in red represent the pixels where the signal is maximum, the minima being represented with black color.

S8. Supporting information 8

TEM, effect of electron beam irradiation and EDAX images

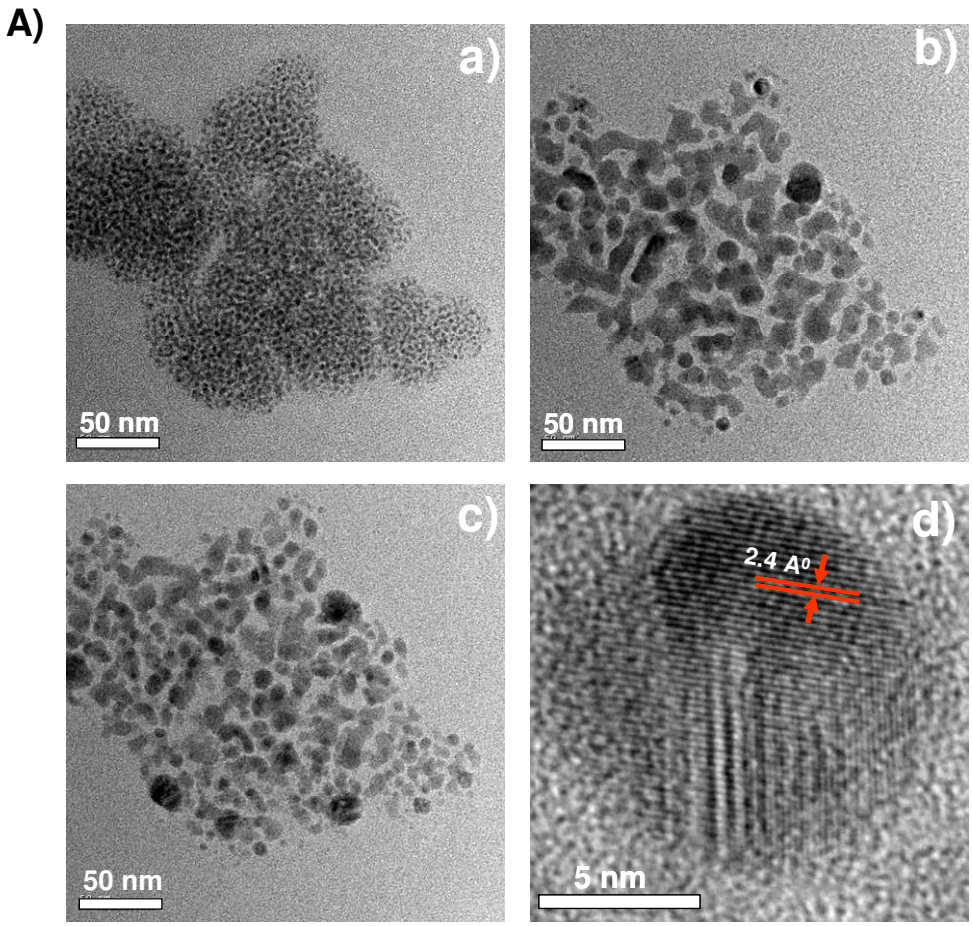

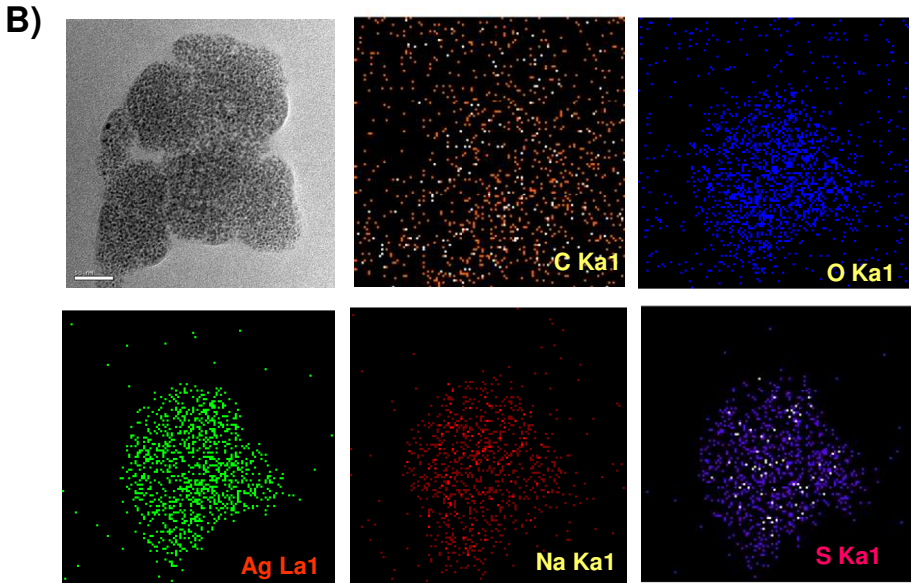

C)

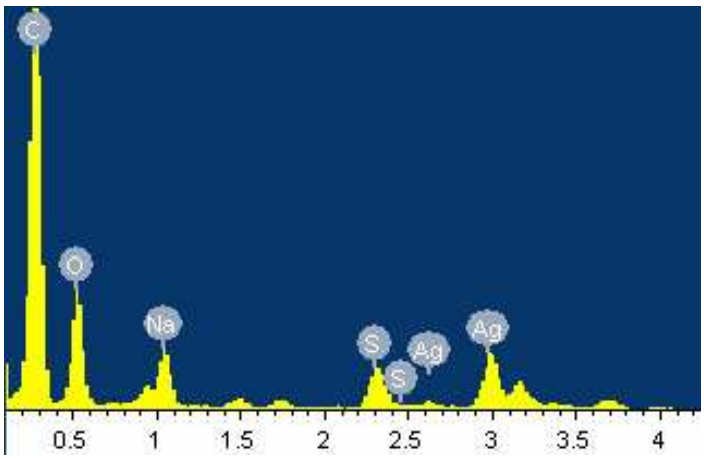

Figure S7. **A)** TEM image of PAGE separated cluster aggregates (I) which upon continuous electron beam irradiation (II) coalesce to form larger nanoparticles. The same regions of the grid are shown in images a, b and c. Image A is at the start of the irradiation showing small clusters, image b is after 10 min. The contrast from the clusters is poor unlike in the case of nanoparticles. In c, the irradiation time is 20 min. Image d is of one grown particle showing the Ag(111) lattice (shown by an arrow). B) TEM image of cluster aggregates for which the EDAX spectrum was taken. EDAX maps using C $\mathbf{K}_{\alpha 1}$, O $\mathbf{K}_{\alpha 1}$, Ag $\mathbf{L}_{\alpha 1}$, Na $\mathbf{K}a_1$ and S $\mathbf{K}_{\alpha 1}$, are shown. C) EDAX spectrum of $Ag_9(H_2MSA)_7$ cluster.

S9. Supporting information 9

Time dependent absorption profiles in water

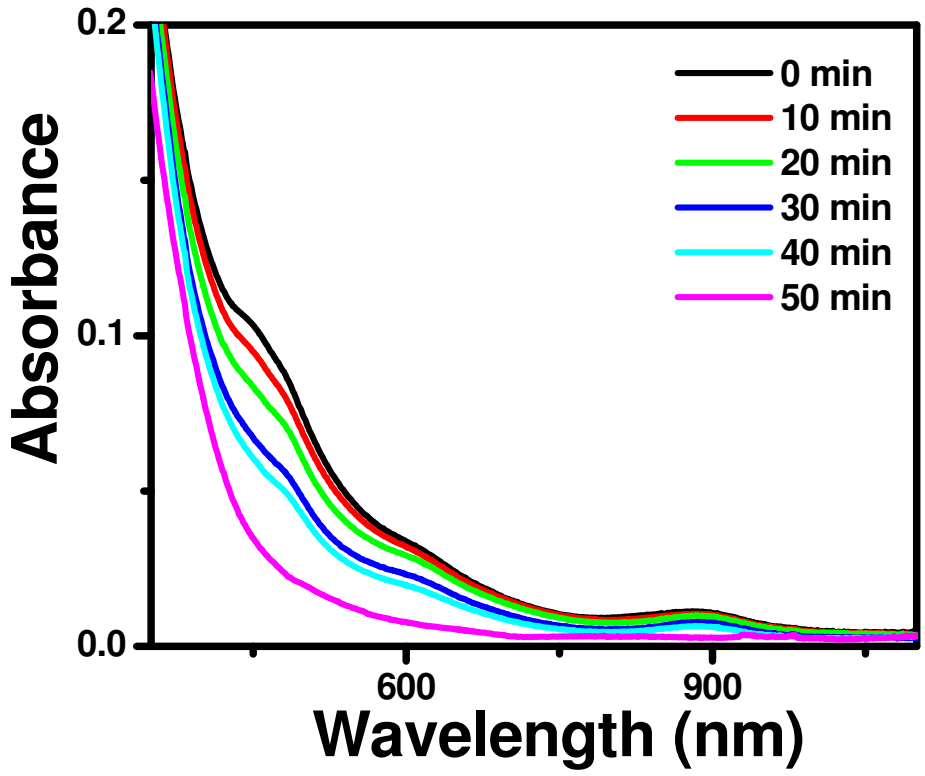

Figure S8. Time dependent UV-Vis spectra of the 5 mg of crude clusters in 3 mL of water, collected at room temperature. There is a gradual reduction in the intensity of the peaks at 886, 625, 489 and 450 nm without change in the position of peaks. Reduction for each the peak intensity occurs at the same rate. Finally a featureless spectrum was observed.

S10. Supporting information 10

Kinetics of decomposition

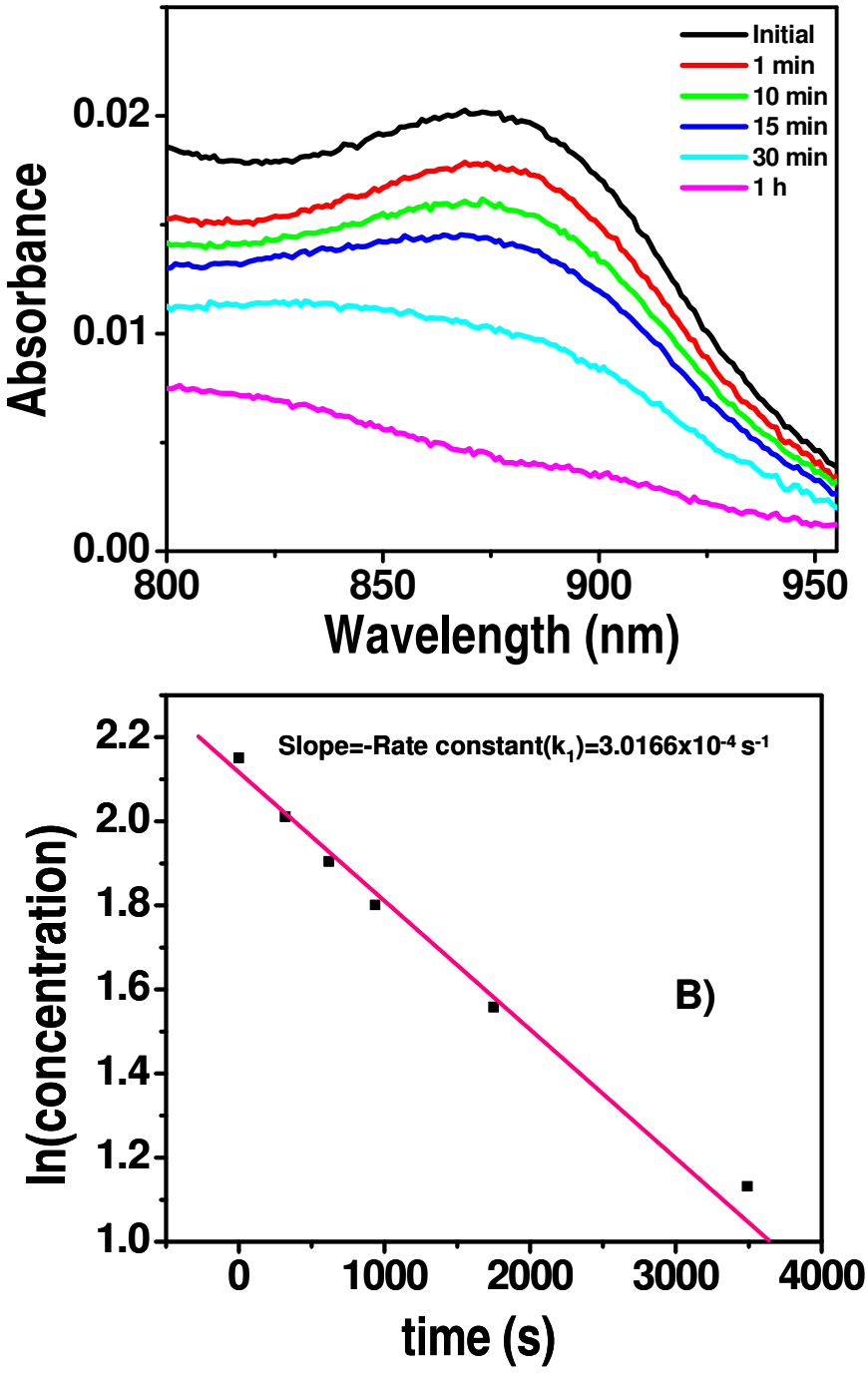

Figure S9. A) Expanded view of the time dependent UV-Vis spectra of the crude cluster in the region of 800-980 nm. Decrease in the intensity and broadening of the peak at 886 nm was observed for 5 mg / 3 mL of H_2O. B) Plot of ln(concentration) Vs time. The intensity of the peak at 886 nm is proportional to concentration.

S11. Supporting information 11

Stability of clusters

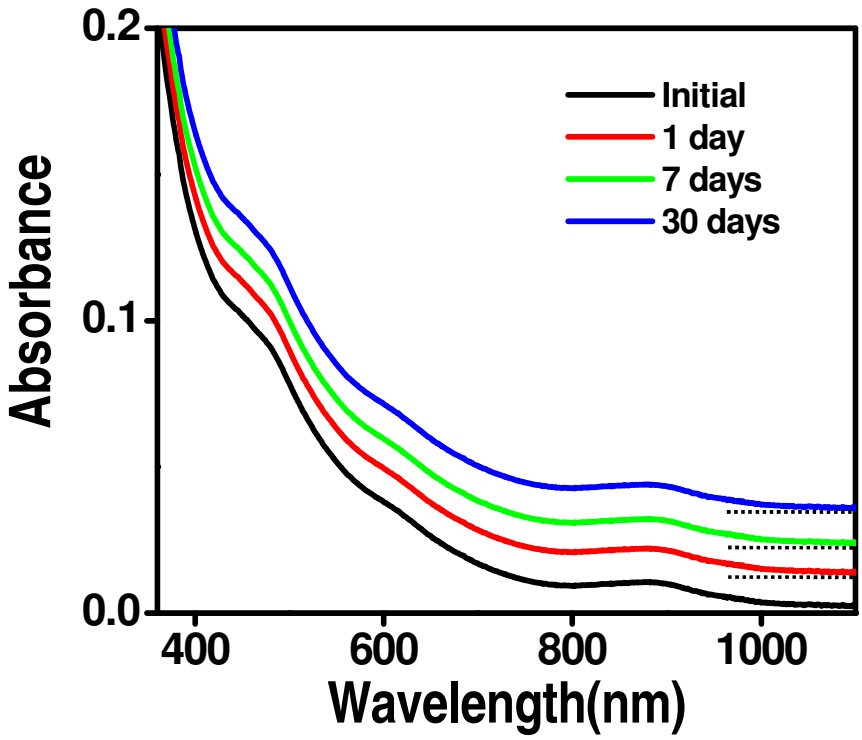

Figure S10. Time dependent UV-Vis spectra of the clusters in (1:1) water:MeOH at pH 8. Traces have been shifted vertically for clarity.

S12. Supporting information 12

Comparison of the ESI MS of the decomposed product with the orange intermediate

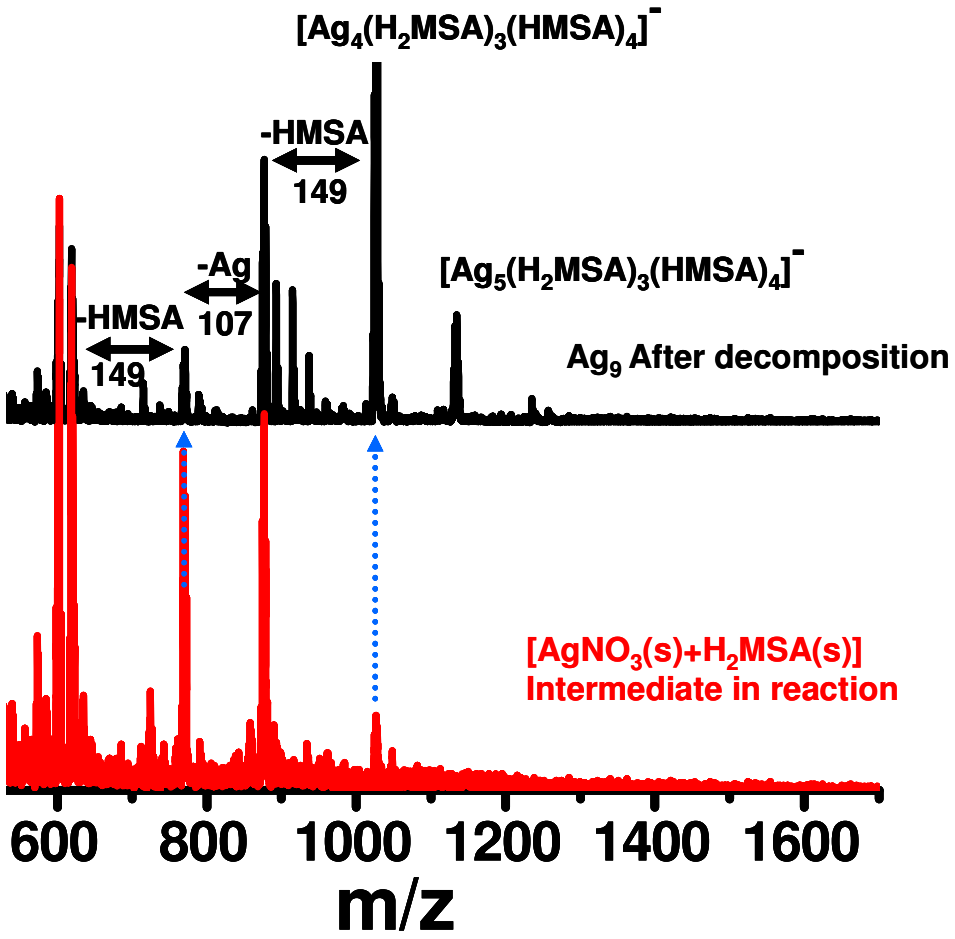

Figure S11. Comparison of the ESI MS of the product of decomposition of Ag_9 cluster with that of the orange colored thiolate formed by mixing $AgNO_3$ and H_2MSA. We observed the common peaks for both compounds. The spectrum of the dissociation product and orange colored thiolate shows typical thiolate peaks. All the ions observed are assigned. The cluster of peaks around m/z 1024, 874, 768 and 619 are due to $Ag_4(H_2MSA)_4^-$ $Ag_4(H_2MSA)_3^-$ $Ag_3(H_2MSA)_3^-$ and $Ag_3(H_2MSA)_2^-$ and their mono- and di- sodium adducts.

S13. Supporting information 13

Expanded ESI MS to show Na addition

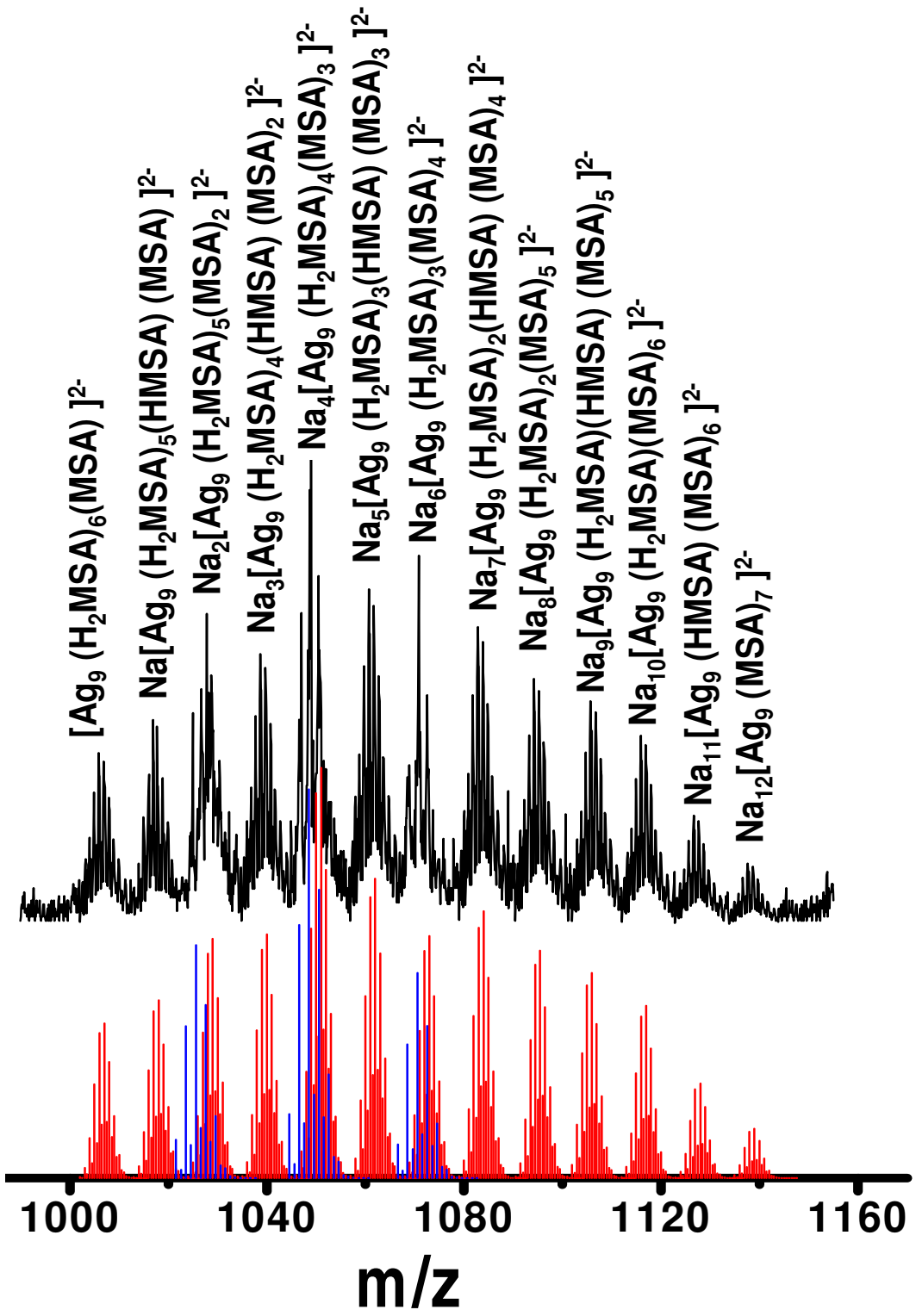

Figure S12. Expanded view of the ESI MS (negative mode) in the m/z 1000-1150 region of the crude cluster mixture. The peaks are assigned. Sodium addition is shown. Sodium arises from $NaBH_4$ used in the synthesis. As H_2MSA is a dicarboxylic acid, it can ionize to give $HMSA^-$ and MSA^{2-}. Each carboxylate ion can pick-up sodium. All the ions observed are assigned. Note that mercaptosuccinic acid on the cluster is in the thiolate form. The cluster of peaks around m/z 1024, 1048, 1068 (in blue) are due to $Ag_4(H_2MSA)_4^-$ and its mono- and di- sodium adducts.

S14. Supporting information 14

MALDI MS

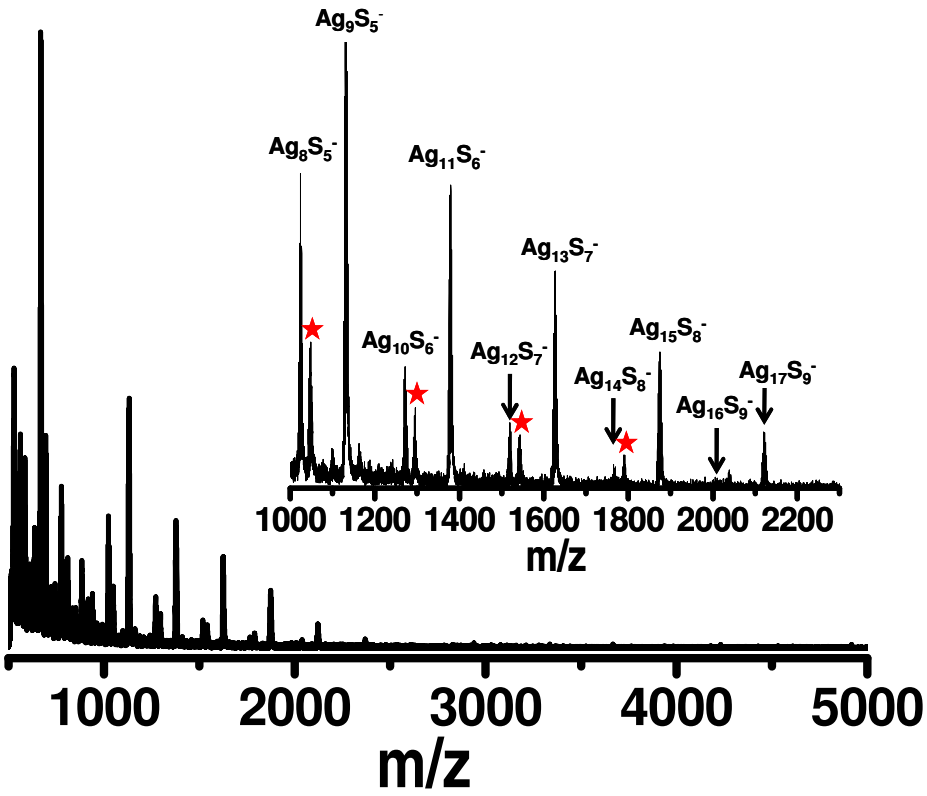

Figure S13. MALDI MS data of PAGE separated clusters. The $Ag_nS_m^-$ series is labeled with their corresponding molecular formulae. Peaks with * show the Na adducts of the preceding formula. Inset shows expanded view of the MALDI MS.

S15. Supporting information 15

XPS

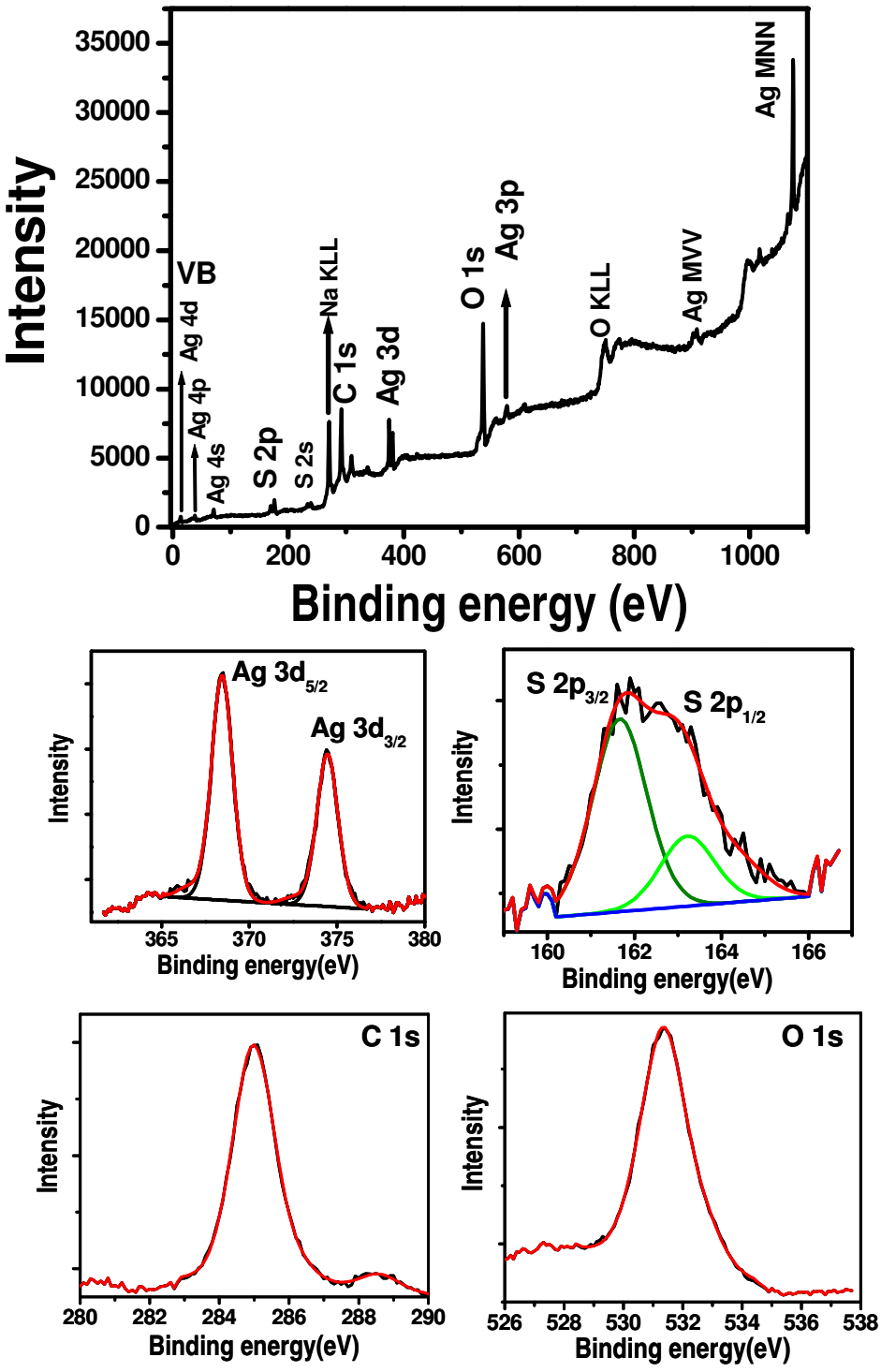

Figure S14. (A) XPS survey spectrum of the as synthesized $Ag_9(H_2MSA)_7$. B, C, D and E are the expanded Ag 3d, S 2p, O 1s and C 1s core level regions, respectively. The Ag:S atomic ratio is 1:0.76 whereas the expected value is 1:0.77. The C:O ratio is not reliable in view of the surface contamination. The S 2p exhibits a thiolate position of 161.8 eV.

S16. Supporting information 16

FT-IR

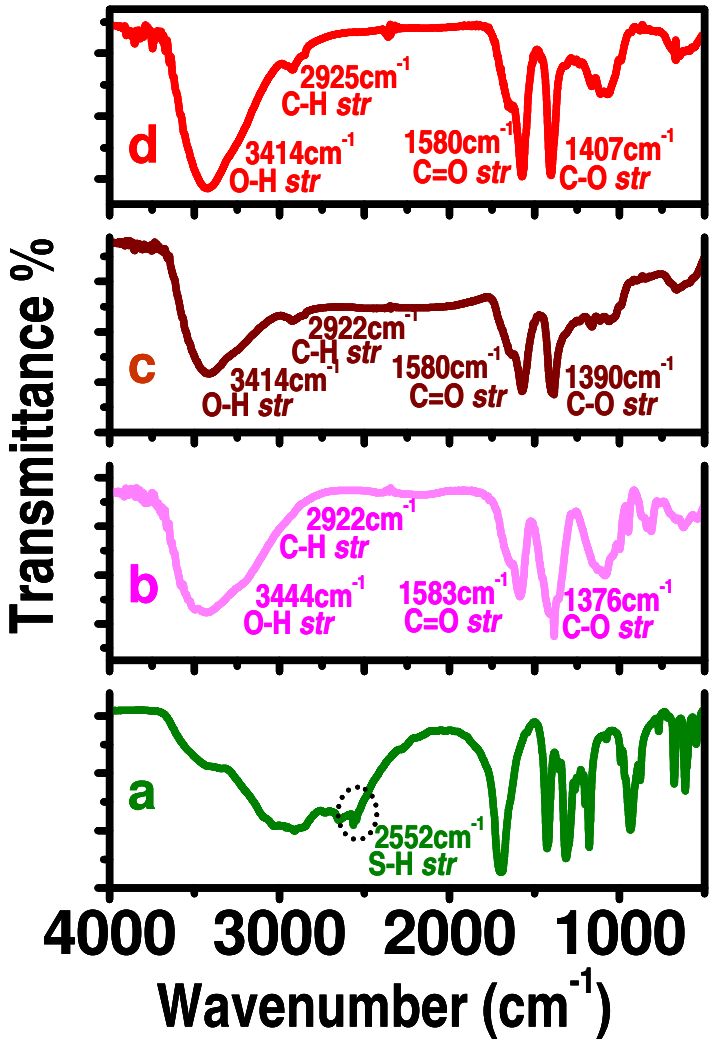

Figure S15. FT-IR spectra of pure (a) H_2MSA, (b) Ag(I)H_2MSA, (c) as-prepared Ag@(H_2MSA) nanoparticles and (d) PAGE separated $Ag_9(H_2MSA)_7$ cluster. The -SH stretching feature at 2552 cm^{-1} in H_2MSA is marked by the dotted-circle in (a) which is absent in other spectra, in agreement with the XPS and mass spectra. H_2MSA features in the region of 2000-500 cm^{-1} confirm the presence of H_2MSA in the cluster. The solid FT-IR spectrum of the $Ag_9(MSA)_7$ cluster showed a strong band at 3450 cm^{-1} due to the hydrated water.

S17. Supporting information 17

EDAX

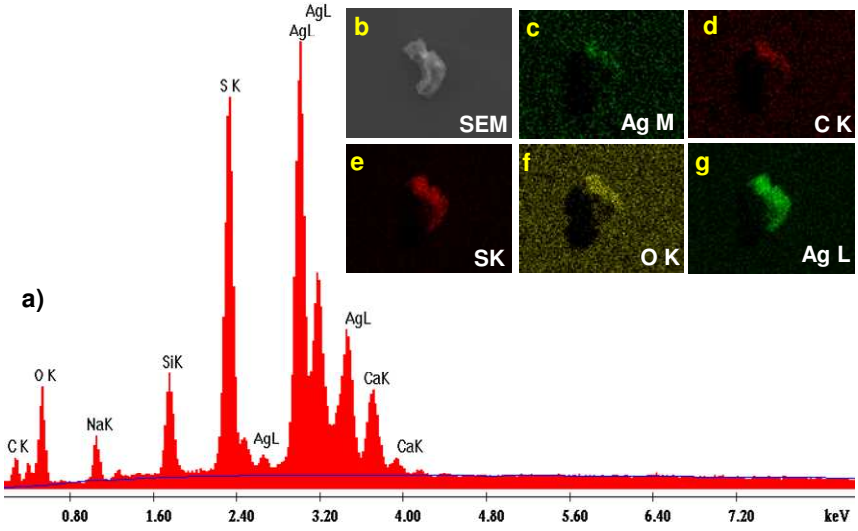

Figure S16. (a) EDAX spectrum of $Ag_9(H_2MSA)_7$ cluster (b) SEM image of the $Ag_9(H_2MSA)_7$ cluster aggregate (PAGE separated) from which the EDAX spectrum was taken. EDAX maps using (c) Ag $\mathbf{M}_\alpha$, (d) C $\mathbf{K}_\alpha$, (e) S $\mathbf{K}_\alpha$, (f) O $\mathbf{K}_\alpha$ and (g) Ag $\mathbf{L}_\alpha$ are shown. Sn $\mathbf{L}_\alpha$, In $\mathbf{L}_\alpha$ and Si $\mathbf{K}_\alpha$ are due to the indium tin oxide substrate used. Ag:S atomic ratio measured is 1:0.75, whereas that expected is 1:0.77.

S18. Supporting information 18

TG analysis

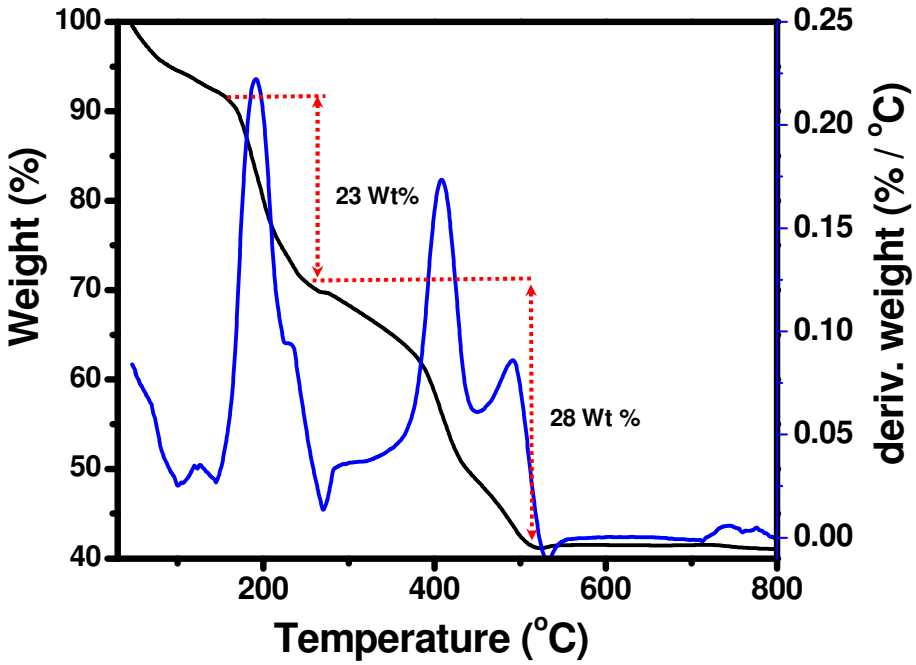

Figure S17. Thermogravimetric (TG) analysis of PAGE separated $Ag_9(H_2MSA)_7$ performed under N_2. Mass loss below 190 °C is attributed to water. Tholate desorption is seen only above 200 °C in monolayer protected silver nanoparticles.[4] This is also reflected in the FT-IR spectra.

S19. Supporting information 19

Elemental analysis of Ag_9 cluster after PAGE separation

Elements	Observed weight%	Expected weight%
C	16.2	16.6
H	4.1	2.0
S	10.8	11.1
N	0.0	0.0
Totals	31.1	29.7

The presence of water cannot be fully eliminated by freeze drying. High temperature drying was not advisable in view of the decomposition. In view of this, elemental analysis is prone to error and the data given show enhancement in H percentage (due to water). However, C and S percentages are as per expectation.

S20. Supporting information 20

XRD at different conditions of synthesis

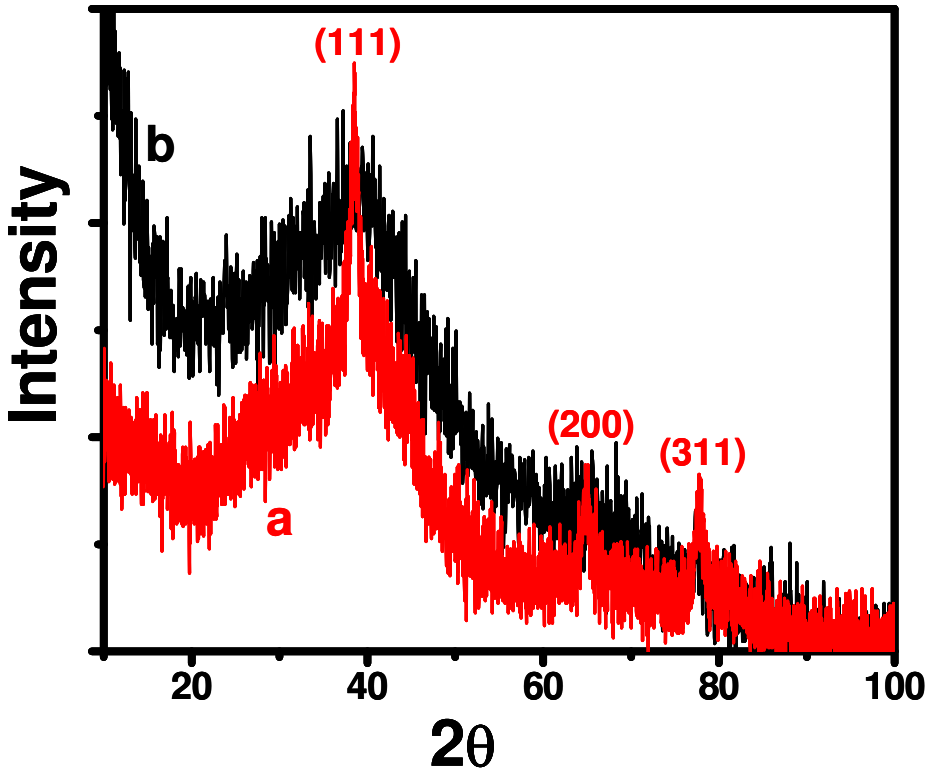

Figure S18. Comparison of the X-ray diffraction patterns of as-synthesized (a) silver nanoparticles at 1:3 silver to thiol ratio using 50 mg of $NaBH_4$ and (b) silver clusters at 1:5 silver to thiol ratio using 50 mg of $NaBH_4$.

S21. Supporting information 21

Cluster synthesis in different solvents

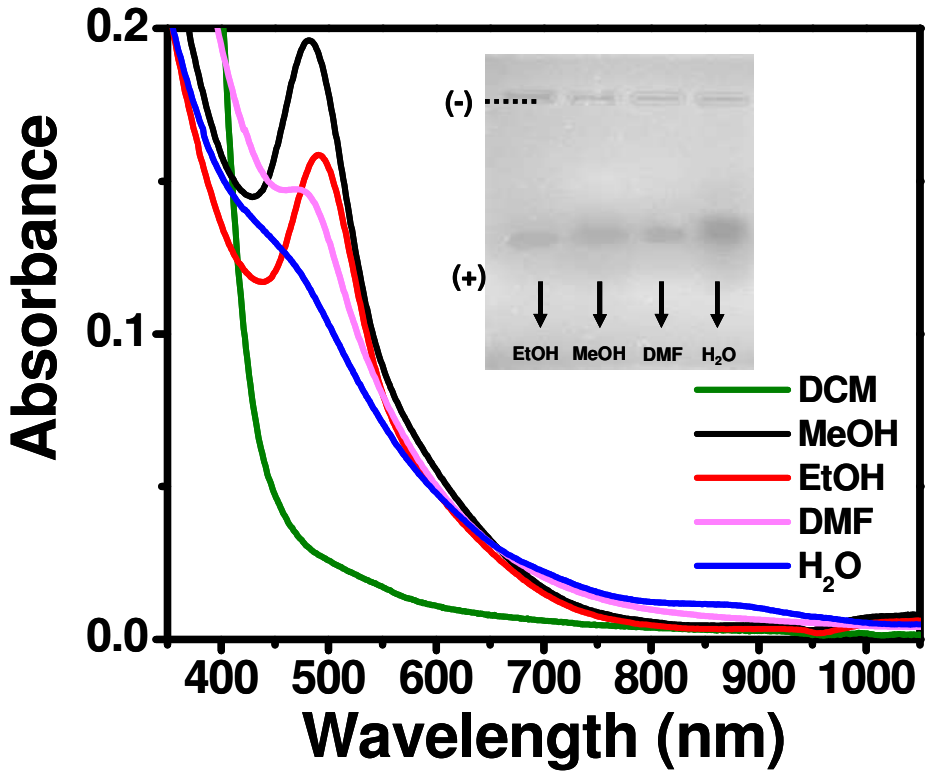

Figure S19. UV-Vis spectra of the clusters synthesized using various solvents**.** The major peak positions are at 530, 480, 490 and 485 nm for dichloromethane, methanol, ethanol and dimethylformamide, respectively. Inset shows an image under UV of an agarose gel on which the samples prepared using a) ethanol, b) methanol, c) DMF and d) H_2O were run.

S22. Supporting information 22

Clusters with different thiols

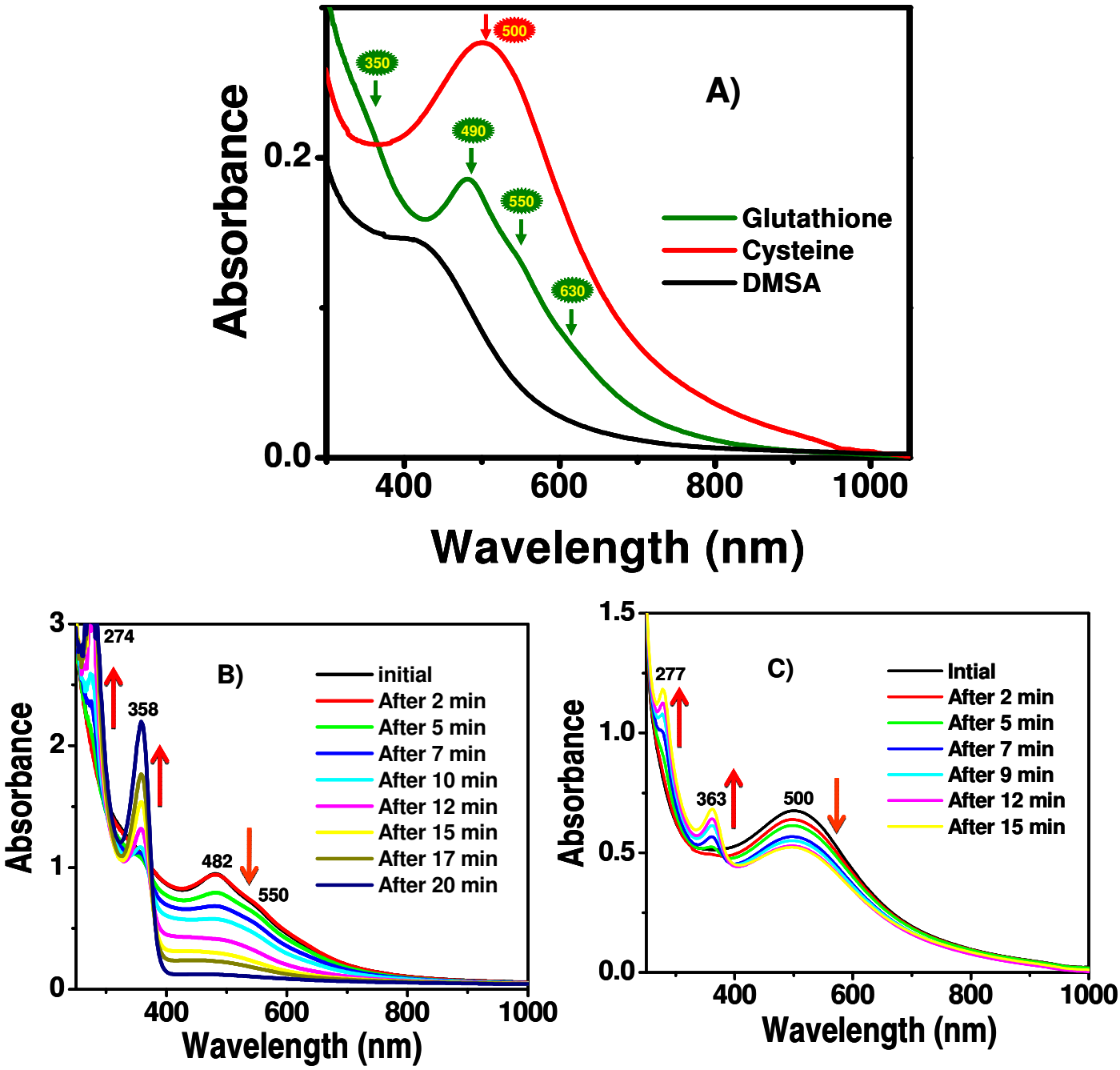

Figure S20. A) UV-Vis spectra of the clusters synthesized using various ligands such as reduced glutathione, cysteine and dimecaptosuccinic acid. B) Time dependent UV-Vis profile of Ag@SG cluster and Ag@cysteine cluster (-SG, glutathione thiolate).

References:

1. Nomiya, K.; Kondoh, Y.; Nagano H.; Oda M. *J. Chem. Soc., Chem. Commun.*, **1995**, 1679.
2. Shibu, E. S.; Habeeb Muhammed, M. A.; Tsukuda, T.; Pradeep. T. *J. Phys. Chem. C* **2008**, *112,* 12168.
3. Nomiya, K.; Onoue, K.-I.; Kondoh, Y.; Kasuga, N. C.; Nagano, H.; Oda. M.; Sakuma, S. Polyhedron, 1995, 14, 1359.
4. N. Sandhyarani, M. P.; Antony, G.; Selvam P.; Pradeep, T. *J. Chem. Phys.*, **2000**, *113,* 9794.